In situ surface laser polishing of laser powder bed fusion 316L steel flat specimens

J.A. Ramos-Grez[1], I. La Fé-Pérdomo[1], Nan Yu[2]
[1] *Pontificia Universidad Católica de Chile, Mechanical and Metallurgical Engineering Department, Av. Vicuña Mackenna 4860 Macul 7820436, Santiago, Chile*
[2] *University of Edinburgh, School of Engineering, Edinburgh, Scotland, United Kingdom*

Abstract

Stainless steel 316L flat specimens were fabricated using a LPBF system (GE Concept Laser MLab 200R) under different sets of process parameters strategies: laser power, layer thickness, scan speed and hatch spacing using N_2 inert atmosphere. Low, medium, and high levels of average surface roughness (10,5 - 17,5 and 22 μm, respectively) were rendered, yet maintaining adequate mechanical properties within nominal values (mass density, ultimate strength, and surface hardness). Flat specimens consisted of 25 mm x 15 mm x 4 mm blocks were fabricated horizontally to assess surface roughness over the fabrication plane. Specimens remained bonded to the build plate during the laser polishing postprocessing to keep position registration as accurate as possible and to remove effects from residual stresses build-up. Laser polishing parameters considered were laser power and scan speed while hatch spacing was kept constant under a fixed scanning pattern strategy; polishing was done under N_2 inert atmosphere using the LPBF system single exposure capability. The as 3D printed roughness and resulting laser polishing roughness measurements were obtained using an optical profilometry scan microscope. Results suggest that it is possible to use the LPBF system to do both fabrication and polishing postprocessing and that an average roughness reduction of up to a 66% can be achieved with a maximum local roughness reduction of 79%. Moreover, mechanisms for surface roughness reduction, namely: surface shallow melting (SSM) and surface over melting (SOM), originally proposed by the main author two decades ago, are observed to operate and explain achieved results.

1 Introduction

Advanced manufacturing is one of the comer stones of the Industry 4.0 (Cunico, 2019). One characteristic of the latter concept is to reduce direct human intervention during the many manufacturing process stages it involves, (Hoffmann, 2019). In this regard, optical energy in the form of a laser beam, is a promising tool to assist and intervene in the human-machine-material interaction (Ready, Farson and Feely, 2001). It is perhaps, the only form of energy that can be modulated in space and time, under atmospheric conditions. This achieved by controlled pulsation at micro, nanosecond and even shorter time duration pulses; as well as, spatial raster scanning from galvanometric actuated mirrors (Steen & Mazumder, 2010). Besides, light does not carry mass, so its inertia is null. Since 1964, high power lasers have been successfully integrated into manufacturing machines for cutting, marking, and welding applications. Other semi-matured technologies based on the laser are that of bending, cladding, texturing and surface heat treatments (Ready, Farson and Feeley, 2001). More recently, during 1990 the development of rapid prototyping technologies marked the start of a new parading in the design and fabrication arena. It was the ultraviolet (UV) and infrared (IR) lasers that were first used at the heart of the SLA (stereolithography) and SLS (selective laser sintering) processes, respectively (Beaman et al., 1997). In later years, several variants of these two processes evolved into successful proof of concepts; today they form the core of the Additive Manufacturing (AM) spectrum of fabricators. Among the latter, the Laser Powder Bed Fusion (LPBF) process known as Selective Laser Melting (SLM), is one of the most commercially successful technologies, as it can 3D print fully dense metallic parts from different material stocks with any degree of shape complexity (Gibson, Rosen and Stucker, 2014). Figure 1 illustrates the LPBF process of a helix fabricated from CoCr powder using a GE-CL MLab 200R unit.

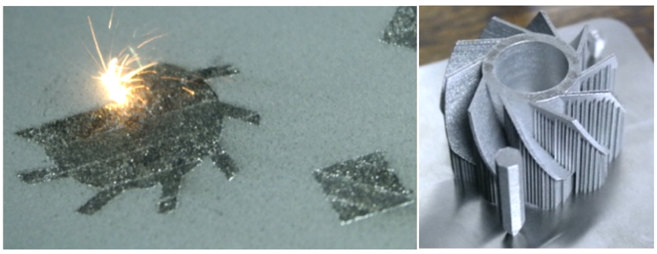

Figure 1: LPBF of cross section of a helix 3D printed in CrCo.

One deleterious feature that pops out immediately from closely observing 3D printed metal part, is its high level of surface roughness (e.g., 10-30 microns peak to trough distance). This somehow unwanted feature is associated with the particle size diameter of the material stock, which commonly ranges between 30 to 60 microns (Ramos et al., 2001). To reduce this roughness, conventional machining techniques have been attempted; however, these are slow and cannot process difficult to reach surface locations (Shi and Gibson, 1998). In that regard, the main author pioneered back in early 2000 on the surface finishing of indirect-SLS metals parts (Ramos and Bourell, 2002). The novelty of this research then was the use of a high-power CO_2 laser, which was raster scanned by galvo actuated mirrors, to laser heat treat the rough surface of the metal 3D printed part to achieve a reduction of up to 37% in the peak to trough valley height. Phenomenological observation then allowed to propose two separate surface smoothing mechanisms: Surface Over Melting (SOM) and Surface Shallow Melting (SSM) (Ramos, Bourell, Beaman, 2003; Ramos-Grez & Bourell, 2004).

1.1 Laser polishing mechanisms

Figure 2 illustrates the flat surface laser polishing strategy proposed in 2004. In Figure 3, schematics of the laser surface melting mechanisms responsible for the surface average roughness reduction are depicted.

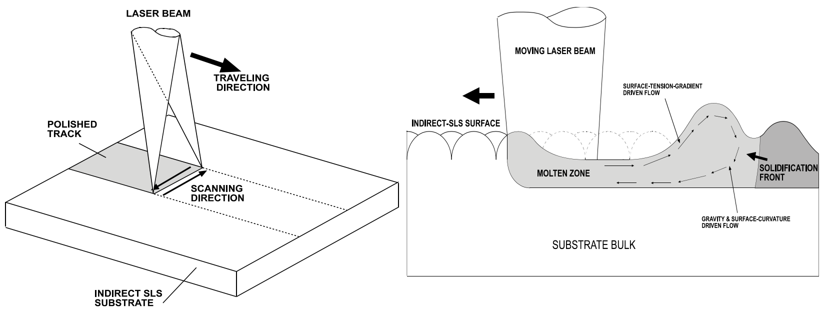

(a) (b)

Figure 2: (a) Schematics of original laser polishing process of a flat specimen (b) Schematic of the laser surface interaction (formation of melt volume, rippling and surface waves evolution). (Ramos et al., 2003)

The SSM and SOM were related to the melting of the surface peaks by the laser fluence which is then followed by the action of surface tension to spread the melt towards the troughs and thus reduce the peak to trough average height as seen in Figure 3. Both mechanisms differed in the amount of surface molten volume, and the thermal gradient induces rippling over the excess melt after becoming solidified leaving the surface with some permanent undulations. Nonetheless, the two mechanisms were shown successful in lowering as 3D printed roughness.

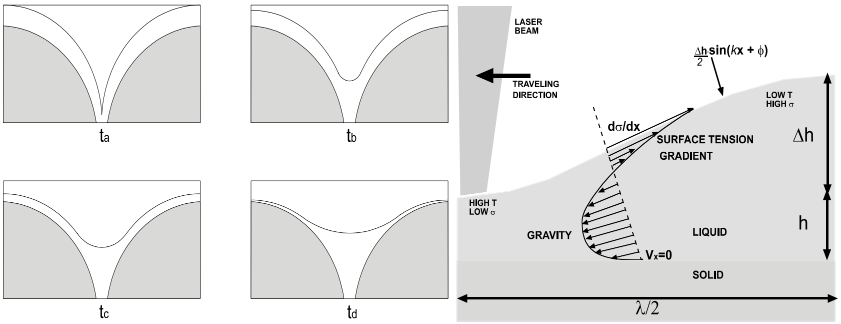

(a) (b)

Figure 3: (a) Sequence of surface melting and spreading towards the trough by capillary action (SSM) (b) Surface ripple formation by thermal capillarity forces (SOM). (Ramos-Grez and Bourell, 2004)

1.2 State of the art since 2004

In 2009, Willenborg and Ostholt (2009) reinforced the fact that re-melting with laser radiation is a method for the automated polishing of 3D surfaces in the tooling industry and medical engineering. One year later, Dadbakhsh, Hao and Kong (2010), performed laser polishing with optimum process parameters set predicted using analytical experimental design. Laser polishing improved the finishing surface of the Laser Material Deposited (LMD) parts to near 2 microns R_a. The relationship of laser energy to final surface roughness showed a strong dependency of surface finish with the former. In 2012, Guo, Hua and Tse (2012), obtained optimum process parameters for the laser polishing in DF2 (AISI 01) tool steel by pulsed Nd:YAG laser. Nüsser, Sändker and Willenborg (2013), investigated the use of an additional laser beam for pre-heating of the surface and the influence of the process parameters on the surface roughness. Bordatchev, Wang et al. (2015), developed a surface prediction model for thermocapillary regime of pulsed laser micro polishing having two distinct polishing regimes: capillary and thermocapillary. The difference between the two regimes is the melt pool flow mechanism. Later, Zhang, Zhou and Shen (2017), determined that the roles of capillary and thermocapillary flow in the process of laser polishing can assist the understanding of the contributions of surface tension (capillary force) and Marangoni effect (thermocapillary force) in the polishing process. This as earlier proposed by Ramos-Grez and Bourell (2004) through the SSM and SOM mechanism, respectively. In Obeidi, McCarthy and O'Connell et al. (2019), AM 316L stainless steel cylindrical samples were polished using CO_2 laser beam irradiation in continuous wave (CW) working mode. A maximum reduction of the roughness from 10,4 to 2,7 µm was achieved. Rosa, Hascoët and Mognol (2020), discussed a methodology to determine laser polishing operating parameters to master the final topography improvement of direct metal deposition parts using the laser polishing process on the same five-axis machine. Hassanin et al. (2021), indicated that both short and long wavelength lasers have been applied for surface polishing to improve the surface finish. Their results showed a reduction in surface roughness of LPBF parts made from AlSiMg powders, from 67%-85% of the as received values. Further in the same line of research, Xu et al. (2021), applied CW laser and a pulsed laser to polish the surface of laser deposition manufactured TiAl alloy samples. These two polishing processes were compared in surface morphology, microstructures, micro-hardness and wear resistance. CW laser polishing of TiAl can reduce roughness near to 1,8 μm, which is comparable to a precisely machined surface.

However, more recently, Gisario, Barletta and Venial (2022), thoroughly reviewed the state of the art signaling that post-processing of AM parts needs to be automated and made scalable so that the technology can be adopted for mass production. Finally, in the field of alternative high energy polishing methods, Metel et al. (2021), have proposed through analytical research a gas-discharge plasma process to finishing laser AM parts, including three processing stages: explosive ablation, polishing with a concentrated beam of fast neutral argon atoms, and coating deposition.

2 Theoretical Framework

Analytical solution to the simplified physical governing equations (i.e., Navier Stokes and energy equations) rendered an algebraic solution for the average peak to trough distance which was then compared and correlated with the experimental results for both Surface Shallow Melting and Surface Over Melting mechanisms (Ramos-Grez and Bourell 2004). These correspond to Equations 1 and 2, respectively and which are presented below. Closed-form analytical expression for the SSM mechanism roughness average value R_a (Equation 1) is a function of the powder radius R, mean powder radius $\overline{R}$, unmelted radius r_m, mean height $\bar{z}$ and filler trough height z_f. Important to notice that the imaginary component of this equation cancels out leaving a real solution. While for the SOM mechanism (Equation 2), a modified solution from Antony and Cline (1977) to the peak-trough distance due to surface rippling of the melt zone is a function of the overheating ΔT of a given depth *h* of the melt pool and the wavelength λ of the ripplings formed.

$$R_a = \frac{\bar{R}}{R_f}\sqrt{r_m^2-\bar{R}^2}-\frac{r_m^2\cdot i}{R_f}\ln\left[\bar{R}\cdot i+\sqrt{r_m^2-\bar{R}^2}\right] + \frac{r_m^2\cdot i}{2R_f}\ln[r_m]-\frac{1}{2}\sqrt{r_m^2-R_f^2}+ \frac{r_m^2\cdot i}{2R_f}\ln\left[R_f\cdot i+\sqrt{r_m^2-R_f^2}\right]+\left(1-\frac{\bar{R}}{R_f}\right)2\bar{z}-z_f \tag{1}$$

$$\Delta h(t) = \frac{3}{2}\frac{\Delta T}{\left(\rho g+\sigma\left(\frac{2\pi}{\lambda}\right)^2\right)h}\cdot\frac{d\sigma}{dT}\cdot e^{\left(-\frac{\mu}{\rho}\cdot\left(\frac{2\pi}{\lambda}\right)^2 t\right)} \tag{2}$$

3 Experimental Set Up

Stainless steel 316L build plates 10x10x10 cm^3 were used to 3D print on them 12 (4x3) rectangular blocks under the same sets of AM process parameters to obtain an average representative roughness value at the build plane surface, Figure 4 (a).

The build plate was then relocated inside the AM machine's processing chamber and its height registered, using a steel recoater blade, to make it coincide with the focal position of the laser beam as illustrated in Figure 4 (b). Following, four sets of laser polishing (LP) parameters were used to laser surface polishing 3 consecutive blocks to attain statistical significance and have an average value representing the modification in surface roughness, Figure 4 (c and d).

The IPG fiber laser of the LPBF system had a wavelength of 1,06 μm and it was focused at 70 μm after passing through a F-theta lens. The scanning pattern was applied along the large axis of the rectangular block at an angle of 67º. Inert atmosphere of N_2 allowed to reduce % O_2 content down to 0,1. The surface roughness of the 3D printed block before and after the laser polishing was then measured using an optical profilometry scan module (OSP470) coupled into a BioLogic's modular M470 scanning electrochemical workstation.

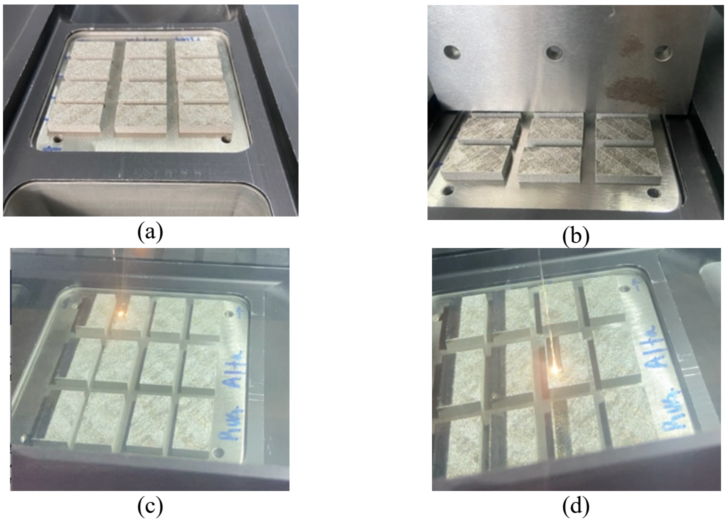

Figure 4: (a) stainless steel 316L build plate with twelve 3D printed specimens of high surface roughness; (b) registration leveling to assure laser beam focal position on specimen's surface; (c) laser polishing of high roughness 1st specimen with 2nd set of parameters (d) laser polishing of high roughness 2nd specimen with 3rd set of parameters.

Table 1 shows printing parameters used for each set of 3D printed blocks and resulting average as-printed roughness.

Table 1: Process parameters used to 3D print blocks with given surface roughness

Laser power (W)	Scan speed (mm/s)	Hatch distance (mm)	Layer thickness (mm)	Energy density (J/mm3)	Average as-printed roughness (mm)
160,0	1000,0	0,07	0,020	114,3	0,01046
160,0	1000,0	0,08	0,030	66,7	0,01750
140,0	1200,0	0,07	0,040	41,7	0,02196

4 Results and Analysis

Figure 5 illustrates the roughness profiles along the longitudinal direction of the 3D printed blocks having an average as-printed roughness of 17 µm (medium AM roughness). The % change in average roughness reduction was computed for each specimen as: $(R_{a3DP} - R_{aLP}) / R_{a3DP}$. It can be noticed that as laser power and scan speed are lowered from 200 W down to 160 W and from 100 mm/s down to 25 mm/s, respectively, a larger % roughness reduction is achieved in this specific set of specimens (from 69% up to 77%). Moreover, Table 2 shows all the recorded surface roughness data from each of the 36 3D printed blocks before and after being surface laser polished, according to the 4 sets of processing parameters used. Average roughness measurements show a 20,3% mean deviation for as-printed surfaces, however the average measurement error for as-polished increases to 37%. Here, % change reduction in average roughness is presented for each set of laser polishing parameters, from which increase in roughness reduction with lower speeds can be verified again as expected, but also with lower laser power, as observed before in Figure 5. This latter result can be counterintuitive, but a high laser power can trigger excessive surface over melt and larger thermal gradients, i.e., more liquid volume formed and higher surface tension, thus larger ripples can be established lowering the roughness reduction.

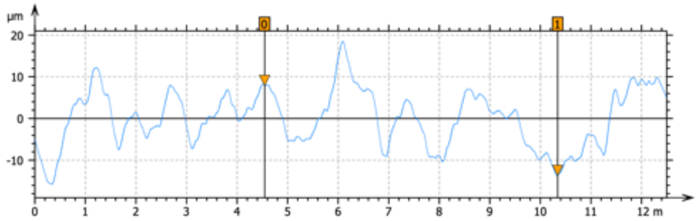

(a) 200 W–100 mm/s;R_a as printed 10,95 µm; R_a as polished 3,43 µm;%Ra reduction 69%.

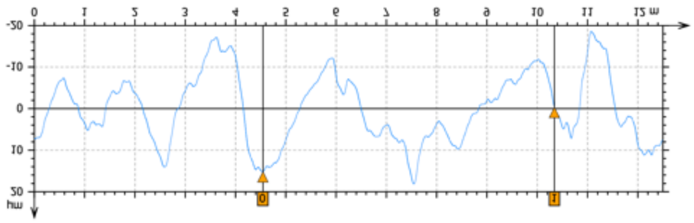

(b) 160 W–25 mm/s;R_a as printed 17,55 µm; R_a as polished 4,09 µm;%R_a reduction 77%.

Figure 5: LP roughness profiles of 3D printed blocks having 17 µm average roughness.

Figure 6 (a)-(d) shows optical macrographs at 20x magnification of the LP tracks performed over the as-printed blocks having the highest AM average surface roughness of 22 µm. From these, it can be noticed that as the scan speed is lowered under both laser powers (200 and 160 W), the undulation appearance is smeared; however, also as the laser power is lowered laser scan tracks are less noticeable.

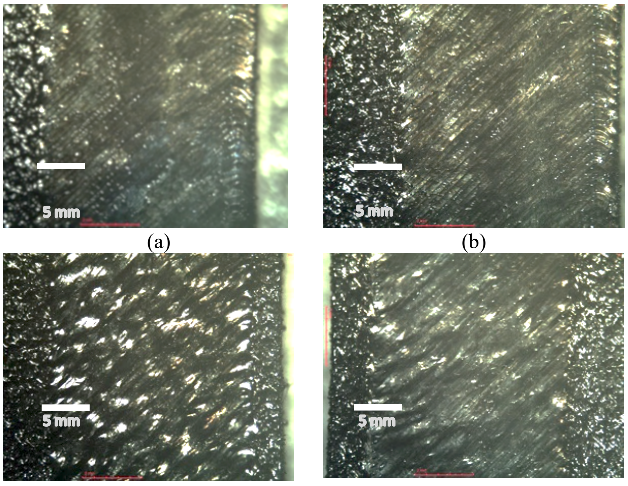

(a) (b) (c) (d)

Figure 6: Macro-optical images taken at 20x of as 3D printed blocks with high AM roughness (22 μm) after laser surface polishing (a) 200 W – 100 mm/s (b) 200 W – 25 mm/s (c) 160 W – 100 mm/s (d) 160 W – 25 mm/s.

Finally, plots of the resulting average surface roughness after laser surface polishing and % roughness reduction are graphed in figures 7 and 8. The latter are plotted as a function of the quotient between the laser power and scan-speed, P/s.s. (i.e., linear energy densities of 1,6 - 2 - 6,4 and 8 J/mm), and with respect to the as-printed surface roughness: High, Medium, and Low, respectively.

Table 2: Experimental roughness results after optical profilometry measurement.

	Low Roughness Ra			Medium Roughness Ra			High Roughness Ra			
Polishing Parameters	As-printed (μm)	As-polished (μm)	Average +/- σ (μm)	As-printed (μm)	As-polished (μm)	Average +/- σ (μm)	As-printed (μm)	As-polished (μm)	Average +/- σ (μm)	% Average Reduction
200 W, 100 mm/s	6,60	6,23	5,34 +/- 0,39	17,90	3,65	3,93+/-0,17	19,84	5,08	5,78+/-0,56	51%
	7,47	4,79		10,95	3,43		23,43	5,20		
	11,33	4,99		15,35	4,71		21,92	7,06		
200 W, 25 mm/s	9,24	1,94	5,53 +/- 1,63	24,45	3,08	4,22+/-0,91	18,42	6,85	3,95+/-1,26	61%
	7,58	6,33		16,90	6,31		18,66	2,18		
	12,12	8,32		14,40	3,27		18,40	2,84		
160 W, 100 mm/s	10,99	4,76	6,95 +/- 1,37	20,98	4,14	10,74+/-3,50	27,24	8,85	8,94+/-0,66	62%
	9,69	6,06		21,62	10,01		26,41	7,67		
	12,31	10,03		21,11	18,07		25,44	10,31		
160 W, 25 mm/s	11,51	5,59	4,08 +/- 0,68	13,11	6,26	5,21+/-0,54	25,09	7,85	5,34+/-1,22	66%
	14,93	3,71		17,55	4,09		19,11	5,20		
	11,71	2,93		15,68	5,28		19,60	2,97		
Average +/- σ (μm)	**10,46+/-1,20**	Average deviation	As-printed 23% As-polished 37%	**17,5+/-1,97**	Average deviation	As-printed 23% As-polished 37%	**21,96+/-1,69**	Average deviation	As-printed 15% As-polished 36%	

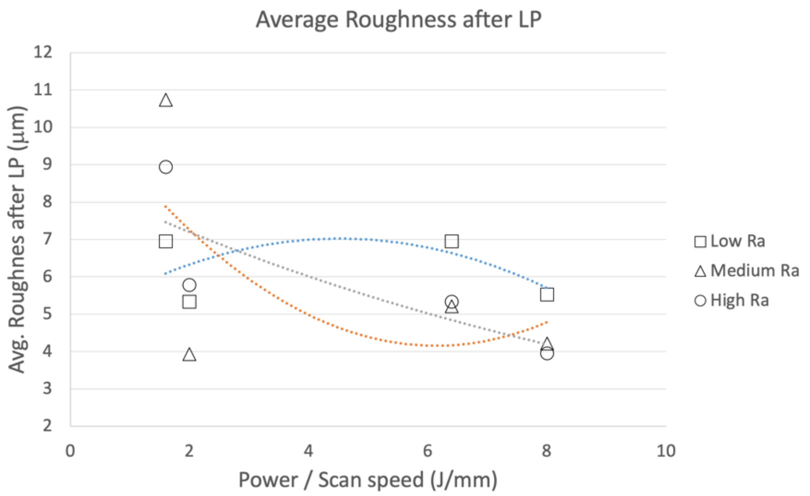

Figure 7: Average roughness after laser polishing vs power/scan-speed for different as-printed roughness values (Low, Medium, High). Shown trends correspond to 2º order polynomials trends.

A common trend is observed in Figure 7 regarding a lower average roughness values achieved as the quotient P/s.s. increases, this for all as-printed average roughness values, having a 2º order polynomial trend. This again is confirmed in Figure 8, where % change reduction in average roughness increases with the P/s.s. ratio, signaling some form of decreasing increments power-law trend. Which in turns augments with increasing as-printed average roughness.

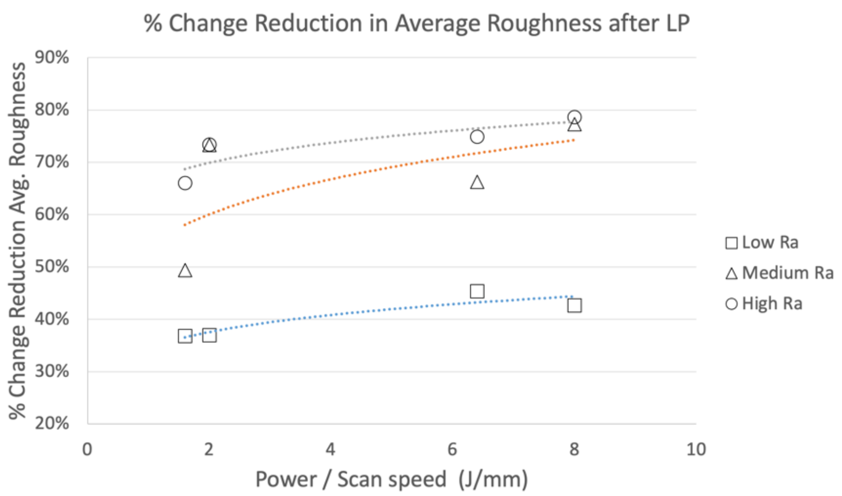

Figure 8: % Change reduction in average roughness after Laser Polishing vs Power/Scan speed for different as-printed roughness values (Low, Medium, High). Shown trends corresponds to power-law.

5 Conclusions

(1) Laser polishing under N_2 inert atmosphere of 3D printed stainless steel 316L parts (i.e., rectangular blocks) was successfully achieved employing the same LPBF system with resulting average surface roughness reduction of up 66%.
(2) Surface roughness reduction is maximized at a combination of both low laser power and scan speed (i.e., linear energy densities of 6,4 and 8,0 J/mm); suggesting that the SOM mechanism operates instead of the SSM, however also at low laser energy density of 1,6 J/mm.
(3) The % change reduction in average surface roughness after the LP process increases with the as-printed surface roughness of the treated specimens.
(4) Average roughness measurement deviation of the laser polished blocks are high (37%) as only three specimens were considered for each set of the 4 processing parameters levels at each of the three as-printed surface roughness.
(5) Laser scan tracks can be seen at high laser power at both low and high scan speed, while at a low laser power surface is smeared as scan speed is lowered.
(6) From the presented literature review, it is observed that the original work initiated in early 2001, has inspired several groups worldwide to keep investigating the laser polishing of parts from different materials and from different laser-based 3D printing methods.
(7) However, to increase % change reduction in surface roughness further, new venues to address the laser polishing process of 3D printed surfaces must be explored. Specifically, employing CW laser processing followed by Quasi-CW or nanoseconds pulsed laser step, individually or in combined modes.

References

1. Cunico, M.W.M. (2019) 3D Printers and Additive Manufacturing: The rise of industry 4.0, 1st edn, Curitiva, Concep3D.
2. Hoffmann, M. (2019) Smart Agents for the Industry 4.0: Enabling Machine Learning in Industrial Production, 1st edn, Springer Verlag.
3. Ready, J.F., Farson, D.F. and Feeley, T. (Eds.) (2001) LIA Handbook of Laser Materials Processing, Laser Institute of America: Magnolia Pub. Inc.
4. Steen, W.M., Mazumder J. (2010) Laser Material Processing, 4th edn, Springer Verlag.
5. Beaman, J.J., Barlow, J.W., Bourell, D.L. and Crawford, R.H. (1997) Solid Freeform Fabrication: A New Direction in Manufacturing,Kluwer Academic.
6. Gibson, I., Rosen, D., Stucker, B. (2014) Additive Manufacturing Technologies: 3D Printing, Rapid Prototyping, and Direct Digital Manufacturing, 1st edn, Springer Verlag.
7. Ramos, J.A., Murphy, J., Wood, K., Bourell, D.L. and Beaman, J.J. (2001) Surface roughness enhancement of indirect-SLS metal parts by laser surface polishing, Proceedings of the SFF Symposium, Vol. 12, pp.28-38.
8. Shi, D. and Gibson, I. (1998) Surface finishing of selective laser sintering parts with robot, Proceedings of the SFF Symposium, Vol. 9, pp.27-35.
9. Ramos, J.A. and Bourell, D.L. (2002) Modelling the surface roughness enhancement of indirect-SLS metal parts after laser surface polishing, in

F.D.S. Marquis and D.L. Bourell (Eds.) Rapid Prototyping of Materials, Warrendale PA: TMS, pp.191-201.
10. Ramos, J.A., Bourell, D.L. and Beaman, J.J. (2003) Surface over-melt during laser polishing of indirect-SLS metal parts, in A. Piqué, A.S. Holmes and D. Dimos (Eds.) Proc. of the 2002 MRS Spring Meeting, Symposium, pp.53-61.
11. Ramos-Grez J. and Bourell D. (2004) Reducing surface roughness of metallic freeform-fabricated parts using non-tactile finishing methods. International Journal of Materials and Product Technology. 21(4), pp. 297-316.
12. Willenborg E. & Ostholt R. (2009) Polishing metals with laser radiation. ILS.
13. Dadbakhsh S., Hao L. and Kong C. (2010) Surface finish improvement of LMD samples using laser polishing Virtual and Physical Prototyping, 5(4).
14. Gou W., Hua M., Tse P. and Mok A. (2021) Process parameters selection for laser polishing DF2 (AISI O1) by Nd:YAG pulsed laser using orthogonal design. The International Journal of Advanced Manufacturing Technology, 59, pp. 1009–1023.
15. Nüsser C., Sändker H. and Willenborg E. (2013) Pulsed laser micro polishing of metals using dual-beam technology. Physics Procedia, 41 pp.346 – 355.
16. Wang Q., Morrow J. and Ma C. (2015) Surface prediction model for thermocapillary regime pulsed laser micro polishing of metals. Journal of Manufacturing Processes, 20.
17. Zhang C., Zhou J. and Shen H. (2017) Role of capillary and thermocapillary forces in laser polishing of metals. Journal of Manufacturing Science and Engineering, Transactions of the ASME, 139(4).
18. Obeidi M., McCarthy E., O'Connell B. et al. (2019) Laser polishing of additive manufactured 316L stainless steel synthesized by selective laser melting. Materials, 12(6).
19. Rosa B., Hascoët J. and Mognol P. (2020) Laser polishing of additive laser manufacturing surfaces: Methodology for parameter setting determination. International Journal of Manufacturing Research, 15(2).
20. El Hassanin A., Obeidi M., Scherillo F., Brabazon D. (2021) CO2 laser polishing of laser-powder bed fusion produced AlSi10Mg parts. Surface and Coatings Technology, 419.
21. Xu Z., Ouyang W., Liu Y., Jiao J., Liu, Y., Zhang W. (2021) Effects of laser polishing on surface morphology and mechanical properties of additive manufactured TiAl components. Journal of Manufacturing Processes, 65.
22. Gisario A., Barletta M. and Veniali F. (2022), Laser polishing: a review of a constantly growing technology in the surface finishing of components made by additive manufacturing The International Journal of Advanced Manufacturing Technology, 120, pp. 1433–1472.
23. Metel A., Grigoriev S., Tarasova T., Melnik Y., Volosova M., Okunkova A., Podrabinnik P., Mustafaev E. (2021) Surface Quality of Metal Parts Produced by Laser Powder Bed Fusion: Ion Polishing in Gas-Discharge Plasma Proposal. Technologies, 9(2).
24. Anthony, T.R. and Cline, H.E. (1977) Surface rippling induced by surface-tension gradients during laser surface melting and alloying, J. Applied Physics, 48, pp. 3888-3894.